EXTENDED EXPERIMENTAL PROCEDURES

B. fragilis Treatment

At 3 weeks of age, saline and poly(I:C) offspring across individual litters were weaned into cages of 4 nonlittermate offspring of the same treatment group to generate a randomized experimental design (Lazic, 2013). Cages within the poly(I:C) versus saline treatment groups were selected at random for treatment with nonenterotoxigenic *B. fragilis* NCTC 9343 (Sears, 2009) or vehicle, every other day for 6 days. To preclude any confounding effects of early life stress on neurodevelopment and behavior, suspensions were not administered by oral gavage. For *B. fragilis* treatment, $10\wedge10$ cfu freshly grown *B. fragilis* was suspended in 1 ml 1.5% sodium bicarbonate, mixed with 4 ml sugar-free applesauce and spread over four standard food pellets. We find that ~42% of *B. fragilis* colony forming units are recovered from the applesauce inoculum at 48 hr after administration, suggesting that both viable and nonviable *B. fragilis* is ingested during the treatment. For vehicle treatment, saline and poly(I:C) animals were fed 1.5% sodium bicarbonate in applesauce over food pellets. Applesauce and pellets were completely consumed by mice of each treatment group by 48 hr after administration. The same procedure was used for treatment with mutant *B. fragilis* lacking PSA and *B. thetaiotaomicron*.

Intestinal qRT-PCR, Western Blots, and Cytokine Profiles

Gut tissue was flushed with HBSS and either (1) homogenized in Trizol for RNA isolation and reverse transcription according to Hsiao and Patterson (2011) or (2) homogenized in Tissue Extraction Reagent I (Invitrogen) containing protease inhibitors (Roche) for protein assays. For cytokine profiling, mouse 20-plex cytokine arrays (Invitrogen) were run on the Luminex FLEXMAP 3D platform by the Clinical Immunobiology Correlative Studies Laboratory at the City of Hope (Duarte, CA). Western blots were conducted according to standard methods and probed with rabbit anti-claudin 8 or rabbit anti-claudin 15 (Invitrogen) at 1:100 dilution.

Microbial DNA Extraction, 16S rRNA Gene Amplification and Pyrosequencing

For each experimental group, 10 mice (5 males, 5 females) from different litters were randomly selected for single housing at weaning and treatment with either vehicle or *B. fragilis*, as described above. Bacterial genomic DNA was extracted from mouse fecal pellets using the MoBio PowerSoil Kit following protocols benchmarked as part of the NIH Human Microbiome Project. The V3-V5 regions of the 16S rRNA gene were PCR amplified using individually barcoded universal primers containing linker sequences for 454-pyrosequencing. Sequencing was performed at the HGSC at BCM using a multiplexed 454-Titanium pyrosequencer.

16S rRNA Gene Sequence Analysis

FASTA and quality files were obtained from the Alkek Center for Metagenomics and Microbiome Research at the Baylor College of Medicine. 16S data were processed and its diversity was analyzed using QIIME 1.6 software package (Caporaso et al., 2010b) as follows. Sequences < 200 bp and > 1,000 bp, and sequences containing any primer mismatches, barcode mismatches, ambiguous bases, homopolymer runs exceeding six bases, or an average quality score of below 30 were discarded and the remaining sequences were checked for chimeras and clustered to operational taxonomic units (OTUs) using the USearch pipeline (Edgar, 2010; Edgar et al., 2011) with a sequence similarity index of 97%. OTUs were subsequently assigned taxonomic classification using the basic local alignment search tool (BLAST) classifier (Altschul et al., 1990), based on the small subunit nonredundant reference database release 111 (Quast et al., 2013) with 0.001 maximum e-value. These taxonomies were then used to generate taxonomic summaries of all OTUs at different taxonomic levels. For tree-based alpha- and beta diversity analyses, representative sequences for each OTU were aligned using PyNAST (Caporaso et al., 2010a) and a phylogenetic tree was constructed based on this alignment using FastTree (Price et al., 2009). Alpha diversity estimates (by Observed Species and Faith's phylogenetic diversity [PD]; Faith, 1992) and evenness (by Simpson's evenness and Gini Coefficient; Wittebolle et al., 2009) were calculated and compared between groups using a nonparametric test based on 100 iterations using a rarefaction of 2,082 sequences from each sample. For beta diversity, even sampling of 2,160 sequences per sample was used, and calculated using weighted and unweighted UniFrac (Lozupone and Knight, 2005). Beta diversity was compared in a pairwise fashion (S versus P, P versus P+BF), from unweighted UniFrac distance matrixes, using the analysis of similarity (ANOSIM; Fierer et al., 2010), permutational multivariate analysis of variance (PERMANOVA; Anderson, 2008; McArdle and Anderson, 2001), permutational analysis of multivariate dispersions (PERMDISP; Anderson et al., 2006), and Moran's I, each with 999 permutations to determine statistical significance.

Identification of Differences in Specific OTUs

Key OTUs, that discriminate between Saline and Poly(I:C) treatment groups, and between Poly(I:C) and Poly(I:C) + *B. fragilis* treatment groups, were identified using an unbiased method from OTU tables, generated by QIIME, using three complimentary analyses: (1) Metastats comparison (White et al., 2009) and (2) the Random Forests algorithm, first under QIIME (Knights et al., 2011) and subsequently coupled with Boruta feature selection, in the Genboree microbiome toolset (Riehle et al., 2012), and (3) the Galaxy platform-based LDA Effect Size analysis (LEfSe; Segata et al., 2011). Only OTUs that differ significantly between treatment groups were candidates for further analyses ($p < 0.05$ for [1] and [3], and > 0.0001 mean decrease in accuracy for Random Forests and subsequent identification by the Boruta algorithm). Metastats analyses were done using the online interface (http://metastats.cbcb.umd.edu) with QIIME-generated OTU tables of any two treatment groups. The Random Forests algorithm was used to identify discriminatory OTUs in the QIIME software package (Breiman, 2001; Knights et al., 2011), comparing two treatment groups at a time,

based on 1,000 trees and a 10-fold cross-validation, and was further validated and coupled with the Boruta feature selection algorithm, as implemented in the Genboree Microbiome toolset (Kursa and Rudnicki, 2010; Riehle et al., 2012). Only those OTUs that were confirmed by the Boruta algorithm were defined as discriminatory. The ratio between observed and calculated error rates was used as a measure of confidence for Random Forests Analyses: this ratio was 5.0 for saline versus poly(I:C) (with an estimated error of 0.1 ± 0.21) and 2.86 for poly(I:C) versus poly(I:C) + *B. fragilis* (with an estimated error of 0.23 ± 0.22). In order to overcome any misidentification by any one of the three methods only OTUs that were identified by at least two of the three above methods were defined as discriminatory. For the analyses in Figure 1 and Table S1, OTUs that were significantly altered by MIA were identified by comparing the saline versus poly(I:C) groups. For the analyses in Figure 3, we compared the poly(I:C) versus poly(I:C)+*B. fragilis* groups, and only report only those OTUs that have also been identified by the analyses in Figure 1 and Table S1. In addition, we compared the results obtained by Random Forests Analysis with feature selection by Boruta to those obtained by Random Forests Analysis with a cutoff of 0.001 mean decrease in accuracy.

To generate a phylogenetic tree depecting the closest cultured type strains to key OTUs identified, key OTUs were than aligned using the SINA aligner (http://www.arb-silva.de/aligner/; (Pruesse et al., 2012), compared to the SILVA reference database release 111 (Quast et al., 2013) using Arb (Ludwig et al., 2004) and visualized using FigTree (http://tree.bio.ed.ac.uk/software/figtree/). Heat maps of key OTUs were generated by extracting their relative abundance from the OTU table. These data were then normalized (so that the sum of squares of all values in a row or column equals one), first by OTU and subsequently by sample, and clustered by correlation using Cluster 3.0 (de Hoon et al., 2004). Finally, abundance data were visualized using Java TreeView (Saldanha, 2004).

Metabolomics Screening

Sera were collected by cardiac puncture from behaviorally validated adult mice. Samples were extracted and analyzed on GC/MS, LC/MS and LC/MS/MS platforms by Metabolon, Inc. Protein fractions were removed by serial extractions with organic aqueous solvents, concentrated using a TurboVap system (Zymark) and vacuum dried. For LC/MS and LC/MS/MS, samples were reconstituted in acidic or basic LC-compatible solvents containing > 11 injection standards and run on a Waters ACQUITY UPLC and Thermo-Finnigan LTQ mass spectrometer, with a linear ion-trap front-end and a Fourier transform ion cyclotron resonance mass spectrometer back-end. For GC/MS, samples were derivatized under dried nitrogen using bistrimethyl-silyl-trifluoroacetamide and analyzed on a Thermo-Finnigan Trace DSQ fast-scanning single-quadrupole mass spectrometer using electron impact ionization. Chemical entities were identified by comparison to metabolomic library entries of purified standards. Following log transformation and imputation with minimum observed values for each compound, data were analyzed using two-way ANOVA with contrasts.

In Vitro Immune Assays

Methods for Treg and Gr-1 flow cytometry and CD4+ T cell in vitro stimulation are described in Hsiao et al. (2012). Briefly, cells were harvested in complete RPMI from spleens and mesenteric lymph nodes. For subtyping of splenocytes, cells were stained with Gr-1 APC, CD11b-PE, CD4-FITC and Ter119-PerCP-Cy5.5 (Biolegend). For detection of Tregs, splenocytes were stimulated for 4 hr with PMA/ionomycin in the presence of GolgiPLUG (BD Biosciences), blocked for Fc receptors and labeled with CD4-FITC, CD25-PE, Foxp3-APC and Ter119-PerCP-Cy5.5. Samples were processed using the FACSCalibur cytometer (BD Biosciences) and analyzed using FlowJo software (TreeStar). For CD4+ T cell stimulation assays, 10∧6 CD4+ T cells were cultured in complete RPMI with PMA (50 ng/ml) and ionomycin (750 ng/ml) for 3 d at 37C with 5% (vol/vol) CO2. Each day, supernatant was collected for ELISA assays to detect IL-6 and IL-17, according to the manufacturer's instructions (eBioscience).

B. fragilis Colonization Assay

Fecal samples were sterilely collected from MIA and control offspring at 1, 2, and 3 weeks after the start of treatment with *B. fragilis* or vehicle. Germ-free mice were treated with *B. fragilis* as described above to serve as positive controls. DNA was isolated from fecal samples using the QIAamp DNA Stool Mini Kit (QIAGEN). 50 ng DNA was used for qPCR with *B. fragilis*-specific, 5′ TGATTCCG CATGGTTTCATT 3′ and 5′ CGACCCATAGAGCCTTCATC 3′, and universal 16S primers 5′ ACTCCTACGGGAGGCAGCAGT 3′ and 5′ ATTACCGCGGCTGCTGGC 3′ according to Odamaki et al. (2008).

Behavioral Testing

Mice were tested beginning at 6 weeks of age for PPI, open field exploration, marble burying, social interaction and adult ultrasonic vocalizations, in that order, with at least 5 days between behavioral tests. Behavioral data for *B. fragilis* treatment and control groups (Figure 5) represent cumulative results collected from multiple litters of 3-5 independent cohorts of mice for PPI and open field tests, 2-4 cohorts for marble burying, 2 cohorts for adult male ultrasonic vocalization and 1 cohort for social interaction. Discrepancies in sample size across behavioral tests reflect differences in when during our experimental study a particular test was implemented.

Prepulse Inhibition

PPI tests are used as a measure of sensorimotor gating and were conducted and analyzed as in Geyer and Swerdlow (2001) and (Smith et al., 2007). Briefly, mice were acclimated to the testing chambers of the SR-LAB startle response system (San Diego Instruments) for 5 min, presented with six 120 db pulses of white noise (startle stimulus) and then subjected to 14 randomized blocks of either no startle, startle stimulus only, 5 db prepulse with startle or 15 db prepulse with startle. The startle response was recorded by a

pliezo-electric sensor, and the percent PPI is defined as: [((startle stimulus only – 5 or 15 db prepulse with startle)/startle stimulus only)*100].

Open field exploration. The open field test is widely used to measure anxiety-like and locomotor behavior in rodents. Mice were placed in 50 × 50 cm white Plexiglas boxes for 10 min. An overhead video camera recorded the session, and Ethovision software (Noldus) was used to analyze the distance traveled, and the number of entries and duration of time spent in the center arena (central 17 cm square).

Marble Burying

Marble burying is an elicited repetitive behavior in rodents analogous to those observed in autistic individuals (Silverman et al., 2010). This test was conducted and analyzed according to methods described in Thomas et al., (2009) and (Malkova et al., 2012). Mice were habituated for 10 min to a novel testing cage containing a 4 cm layer of chipped cedar wood bedding and then transferred to a new housing cage. 18 glass marbles (15 mm diameter) were aligned equidistantly 6 × 3 in the testing cage. Mice were returned to the testing cage and the number of marbles buried in 10 min was recorded.

Sociability and Social Preference

Social interaction tests were conducted and analyzed according to methods adopted from Sankoorikal et al. (2006) and (Yang et al., 2011). Briefly, testing mice were habituated for 10 min to a 50 × 75 cm Plexiglas three-chambered apparatus containing clear interaction cylinders in each of the side chambers. Sociability was tested in the following 10 min session, where the testing mouse was given the opportunity to explore a novel same-sex, age-matched mouse in one interaction cylinder (social object) versus a novel toy (green sticky ball) in the other interaction cylinder of the opposite chamber. Social preference was tested in the final 10 min session, where the testing mouse was given the opportunity to explore a now familiar mouse (stimulus mouse from the previous sociability session) versus a novel unfamiliar same-sex, age-matched mouse. In each session, the trajectory of the testing mouse was tracked with Ethovision software (Noldus). Sociability data are presented as preference for the mouse over the toy: percent of time in the social chamber - percent of time in the nonsocial chamber, and social preference data are presented as preference for the unfamiliar mouse over the familiar mouse: percent of time in the unfamiliar mouse chamber—percent of time in the familiar mouse chamber. Similar indexes were measured for chamber entries, and entries into and duration spent in the contact zone (7 × 7 cm square surrounding the interaction cylinder).

Adult Ultrasonic Vocalizations

Male mice produce USVs in response to female mice as an important form of communication (Portfors, 2007). We measured adult male USV production in response to novel female exposure according to methods described in Grimsley et al. (2011), Scattoni et al. (2011), and Silverman et al. (2010). Adult males were single-housed one week before testing and exposed for 20 min to an unfamiliar adult female mouse each day starting four days prior to testing in order to provide a standardized history of sexual experience and to adjust for differences in social dominance. On testing day, mice were habituated to a novel cage for 10 min before exposure to a novel age-matched female. USVs were recorded for 3 min using the UltraSoundGate microphone and audio system (Avisoft Bioacoustics). Recordings were analyzed using Avisoft's SASLab Pro software after fast Fourier transformation at 512 FFT-length and detection by a threshold-based algorithm with 5 ms hold time. Data presented reflect duration and number of calls produced in the 3 min session.

4EPS Synthesis and Detection

Potassium 4-ethylphenylsulfate was prepared using a modification of a procedure reported for the synthesis of aryl sulfates in Burlingham et al. (2003) and Grimes (1959) (Figure S7A). 4-ethylphenol (Sigma-Aldrich, 5.00 g, 40.9 mmol) was treated with sulfur trioxide-pyridine complex (Sigma-Aldrich, 5.92 g, 37.2 mmol) in refluxing benzene (20 ml, dried by passing through an activated alumina column). After 3.5 hr, the resulting solution was cooled to room temperature, at which point the product crystallized. Isolation by filtration afforded 7.93 g of crude pyridinium 4-ethylphenylsulfate as a white crystalline solid. 1.00 g of this material was dissolved in 10 ml of 3% triethylamine in acetonitrile and filtered through a plug of silica gel (Silicycle, partical size 32-63 μm), eluting with 3% triethylamine in acetonitrile. The filtrate was then concentrated, and the resulting residue was dissolved in 20 ml of deionized water and eluted through a column of Dowex 50WX8 ion exchange resin (K+ form), rinsing with 20 ml of deionized water. The ion exchange process was repeated once more, and the resulting solution concentrated under vacuum to afford 618 mg (55% overall yield) of potassium 4-ethylphenylsulfate as a white powder (Figure S7A).

1H and 13C NMR spectra of authentic potassium 4-ethylphenylsulfate were recorded on a Varian Inova 500 spectrometer and are reported relative to internal DMSO-d_5 (1H, $\delta = 2.50$; 13C, $\delta = 39.52$). A high-resolution mass spectrum (HRMS) was acquired using an Agilent 6200 Series TOF with an Agilent G1978A Multimode source in mixed ionization mode (electrospray ionization [ESI] and atmospheric pressure chemical ionization [APCI]). Spectroscopic data for potassium 4-ethylphenylsulfate are as follows: 1H NMR (DMSO-d_6, 500 MHz) δ 7.11 – 7.04 (m, 4H), 2.54 (q, $J = 7.6$ Hz, 2H), 1.15 (t, $J = 7.6$ Hz, 3H); 13C NMR (DMSO-d_6, 126 MHz) δ 151.4, 138.3, 127.9, 120.6, 27.5, 16.0; HRMS (Multimode-ESI/APCI) calculated for C8H9O4S [M–K]- 201.0227, found 201.0225.

Authentic 4EPS and serum samples were analyzed by LC/MS using an Agilent 110 Series HPLC system equipped with a photodiode array detector and interfaced to a model G1946C single-quadrupole expectospray mass spectrometer. HPLC separations were obtained at 25°C using an Agilent Zorbax XDB-C18 column (4.6 mm × 50 mm × 5 um particle size). The 4EPS ion was detected using selected ion monitoring for ions of m/z 200.9 and dwell time of 580 ms/ion, with the electrospray capillary set at 3 kV. Authentic potassium 4EPS was found to possess a retention time of 6.2 min when eluted in 0.05% trifluoroacetic acid and acetonitrile, using a 10 min linear gradient from 0%–50% acetonitrile. For quantification of 4EPS in mouse sera, a dose-response curve was constructed

by plotting the total ion count peak area for known concentrations of authentic potassium 4EPS against the analyte concentration (R∧2 = 0.9998; Figure S7B). Mouse serum samples were diluted 4-fold with acetonitrile and centrifuged at 10,000 g at 4°C for 3 min. 10 ul of supernatant was injected directly into the HPLC system.

SUPPLEMENTAL REFERENCES

Anderson, M.J. (2008). A new method for non-parametric multivariate analysis of variance. Austral Ecol. *26*, 32–46.

Breiman, L. (2001). Random forests. Mach. Learn. *45*, 5–32.

Burlingham, B.T., Pratt, L.M., Davidson, E.R., Shiner, V.J., Jr., Fong, J., and Widlanski, T.S. (2003). 34S isotope effect on sulfate ester hydrolysis: mechanistic implications. J. Am. Chem. Soc. *125*, 13036–13037.

Caporaso, J.G., Bittinger, K., Bushman, F.D., DeSantis, T.Z., Andersen, G.L., and Knight, R. (2010a). PyNAST: a flexible tool for aligning sequences to a template alignment. Bioinformatics *26*, 266–267.

Caporaso, J.G., Kuczynski, J., Stombaugh, J., Bittinger, K., Bushman, F.D., Costello, E.K., Fierer, N., Peña, A.G., Goodrich, J.K., Gordon, J.I., et al. (2010b). QIIME allows analysis of high-throughput community sequencing data. Nat. Methods *7*, 335–336.

de Hoon, M.J.L., Imoto, S., Nolan, J., and Miyano, S. (2004). Open source clustering software. Bioinformatics *20*, 1453–1454.

Edgar, R.C. (2010). Search and clustering orders of magnitude faster than BLAST. Bioinformatics *26*, 2460–2461.

Edgar, R.C., Haas, B.J., Clemente, J.C., Quince, C., and Knight, R. (2011). UCHIME improves sensitivity and speed of chimera detection. Bioinformatics *27*, 2194–2200.

Faith, D.P. (1992). Conservation Evaluation and Phylogenetic Diversity. Biol. Conserv. *61*, 1–10.

Geyer, M.A., and Swerdlow, N.R. (2001). Measurement of startle response, prepulse inhibition, and habituation. Curr Protoc Neurosci *Chapter 8*, Unit 8 7.

Grimes, A.J. (1959). Synthesis of 35S-labelled arylsulphates byintact animals and by tissue preparations, with particular reference to L-tyrosine O-sulphate. Biochem. J. *73*, 723–729.

Hsiao, E.Y., McBride, S.W., Chow, J., Mazmanian, S.K., and Patterson, P.H. (2012). Modeling an autism risk factor in mice leads to permanent immune dysregulation. Proc. Natl. Acad. Sci. USA *109*, 12776–12781.

Hsiao, E.Y., and Patterson, P.H. (2011). Activation of the maternal immune system induces endocrine changes in the placenta via IL-6. Brain Behav. Immun. *25*, 604–615.

Knights, D., Costello, E.K., and Knight, R. (2011). Supervised classification of human microbiota. FEMS Microbiol. Rev. *35*, 343–359.

Kursa, M.B., and Rudnicki, W.R. (2010). Feature Selection with the Boruta Package. J. Stat. Softw. *36*, 1–13.

Lazic, S.E. (2013). Comment on "Stress in puberty unmasks latent neuropathological consequences of prenatal immune activation in mice". Science *340*, 811.

Lozupone, C., and Knight, R. (2005). UniFrac: a new phylogenetic method for comparing microbial communities. Appl. Environ. Microbiol. *71*, 8228–8235.

Ludwig, W., Strunk, O., Westram, R., Richter, L., Meier, H., Yadhukumar, Buchner, A., Lai, T., Steppi, S., Jobb, G., et al. (2004). ARB: a software environment for sequence data. Nucleic Acids Res. *32*, 1363–1371.

McArdle, B.H., and Anderson, M.J. (2001). Fitting multivariate models to community data: a comment on distancebased redundancy analysis. Ecology *82*, 290–297.

Odamaki, T., Xiao, J.Z., Sakamoto, M., Kondo, S., Yaeshima, T., Iwatsuki, K., Togashi, H., Enomoto, T., and Benno, Y. (2008). Distribution of different species of the Bacteroides fragilis group in individuals with Japanese cedar pollinosis. Appl. Environ. Microbiol. *74*, 6814–6817.

Portfors, C.V. (2007). Types and functions of ultrasonic vocalizations in laboratory rats and mice. J. Am. Assoc. Lab. Anim. Sci. *46*, 28–34.

Price, M.N., Dehal, P.S., and Arkin, A.P. (2009). FastTree: computing large minimum evolution trees with profiles instead of a distance matrix. Mol. Biol. Evol. *26*, 1641–1650.

Pruesse, E., Peplies, J., and Glöckner, F.O. (2012). SINA: accurate high-throughput multiple sequence alignment of ribosomal RNA genes. Bioinformatics *28*, 1823–1829.

Quast, C., Pruesse, E., Yilmaz, P., Gerken, J., Schweer, T., Yarza, P., Peplies, J., and Glöckner, F.O. (2013). The SILVA ribosomal RNA gene database project: improved data processing and web-based tools. Nucleic Acids Res. *41* (Database issue), D590–D596.

Riehle, K., Coarfa, C., Jackson, A., Ma, J., Tandon, A., Paithankar, S., Raghuraman, S., Mistretta, T.A., Saulnier, D., Raza, S., et al. (2012). The Genboree Microbiome Toolset and the analysis of 16S rRNA microbial sequences. BMC Bioinformatics *13* (*Suppl 13*), S11.

Saldanha, A.J. (2004). Java Treeview—extensible visualization of microarray data. Bioinformatics *20*, 3246–3248.

Sankoorikal, G.M., Kaercher, K.A., Boon, C.J., Lee, J.K., and Brodkin, E.S. (2006). A mouse model system for genetic analysis of sociability: C57BL/6J versus BALB/cJ inbred mouse strains. Biol. Psychiatry *59*, 415–423.

Scattoni, M.L., Ricceri, L., and Crawley, J.N. (2011). Unusual repertoire of vocalizations in adult BTBR T+tf/J mice during three types of social encounters. Genes Brain Behav. *10*, 44–56.

Sears, C.L. (2009). Enterotoxigenic Bacteroides fragilis: a rogue among symbiotes. Clin. Microbiol. Rev. *22*, 349–369.

Segata, N., Izard, J., Waldron, L., Gevers, D., Miropolsky, L., Garrett, W.S., and Huttenhower, C. (2011). Metagenomic biomarker discovery and explanation. Genome Biol. *12*, R60.

White, J.R., Nagarajan, N., and Pop, M. (2009). Statistical methods for detecting differentially abundant features in clinical metagenomic samples. PLoS Comput. Biol. *5*, e1000352.

Wittebolle, L., Marzorati, M., Clement, L., Balloi, A., Daffonchio, D., Heylen, K., De Vos, P., Verstraete, W., and Boon, N. (2009). Initial community evenness favours functionality under selective stress. Nature *458*, 623–626.

Yang, M., Silverman, J.L., and Crawley, J.N. (2011). Automated three-chambered social approach task for mice. Curr Protoc Neurosci *Chapter 8*, Unit 8 26.

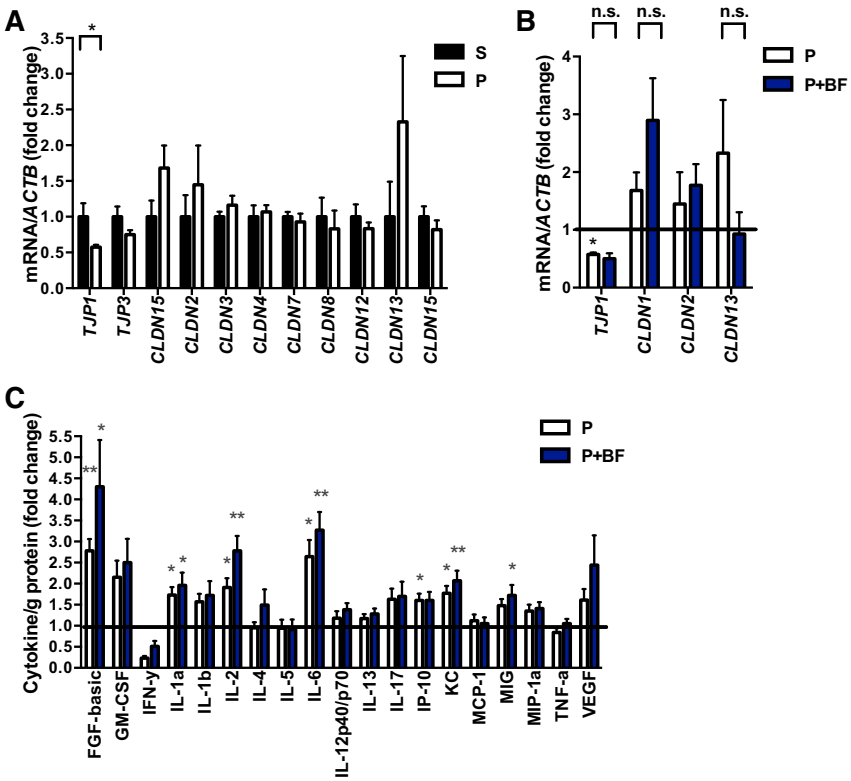

Figure S1. *B. fragilis* Treatment Has Little Effect on Tight Junction Expression and Cytokine Profiles in the Small Intestine, Related to Figures 1 and 3

(A) Expression of tight junction components relative to β-actin in small intestines of adult saline and poly(I:C) offspring. Data for each gene are normalized to expression levels in saline offspring. n = 8/group.

(B) Quantification of the effect of *B. fragilis* treatment on expression of notable tight junction components relative to β-actin in small intestines of MIA offspring. Data for saline and poly(I:C) are as in (A). n = 8/group.

(C) Protein levels of cytokines and chemokines relative to total protein content in small intestines of adult saline, poly(I:C) and poly(I:C)+*B. fragilis* offspring. Data are normalized to expression levels in saline offspring. Asterisks directly above bars indicate significance compared to saline control (normalized to 1, as denoted by the black line), whereas asterisks at the top of the graph denote statistical significance between poly(I:C) and poly(I:C)+*B. fragilis* groups. n = 8-10/group.

Data are presented as mean ± SEM. *p < 0.05, **p < 0.01, S = saline+vehicle, p = poly(I:C)+vehicle, P+BF = poly(I:C)+*B. fragilis*.

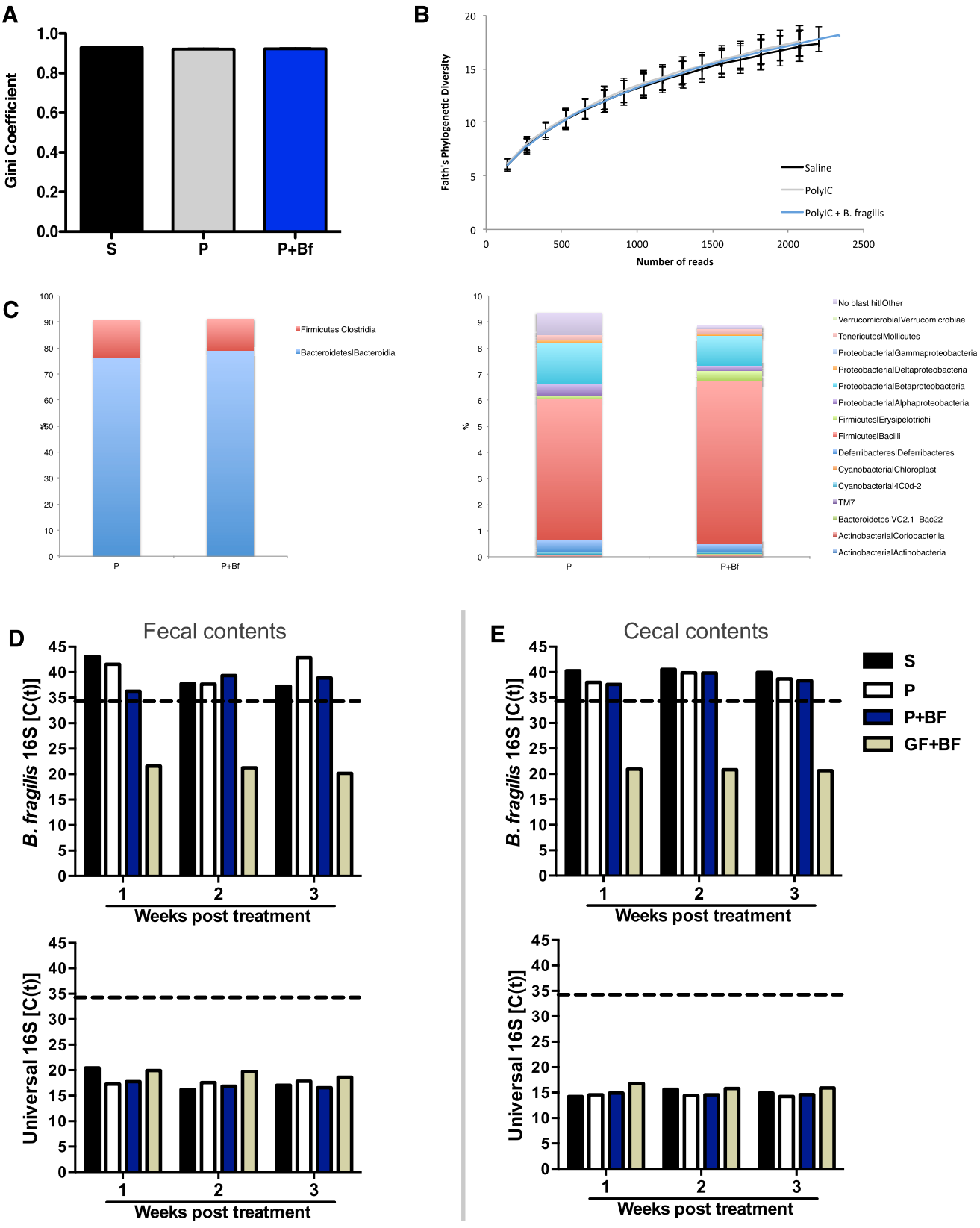

(legend on next page)

Figure S2. No Evidence for Persistent Colonization of *B. fragilis* after Treatment of MIA Offspring, Related to Figures 2 and 4

(A) Evenness of the gut microbiota, as indicated by the Gini coefficient. n = 10/group.

(B) Richness of the gut microbiota, as illustrated by rarefaction curves plotting Faith's Phylogenetic Diversity (PD) versus the number of sequences for each treatment group. n = 10/group.

(C) Mean relative abundance of OTUs classified by taxonomic assignments at the class level for the most abundant taxa (left) and least abundant taxa (right) for poly(I:C) versus poly(I:C)+*B. fragilis* treatment. n = 10/group.

(D) Levels of *B. fragilis* 16S sequence (top) and bacterial 16S sequence (bottom) in fecal samples collected at 1, 2, and 3 weeks posttreatment of adult offspring with vehicle or *B. fragilis*. Germ-free mice colonized with *B. fragilis* were used as a positive control. Data are presented as quantitative RT-PCR cycling thresholds [C(t)], where C(t) > 34 (hatched line) is considered negligible, and for C(t) < 34, lesser C(t) equates to stronger abundance. n = 1, where each represents pooled sample from 3-5 independent cages.

(E) Levels of *B. fragilis* 16S sequence (top) and bacterial 16S sequence (bottom) in cecal samples collected at 1, 2, and 3 weeks posttreatment of adult offspring with vehicle or *B. fragilis*. Germ-free mice colonized with *B. fragilis* were used as a positive control. Data are presented as quantitative RT-PCR cycling thresholds [C(t)], where C(t) > 34 (hatched line) is considered negligible, and for C(t) < 34, lesser C(t) equates to stronger abundance. n = 1, where each represents pooled sample from 3-5 independent cages.

Data are presented as mean ± SEM. S = saline+vehicle, p = poly(I:C)+vehicle, P+BF = poly(I:C)+*B. fragilis*, GF+BF = germ-free+*B. fragilis*.

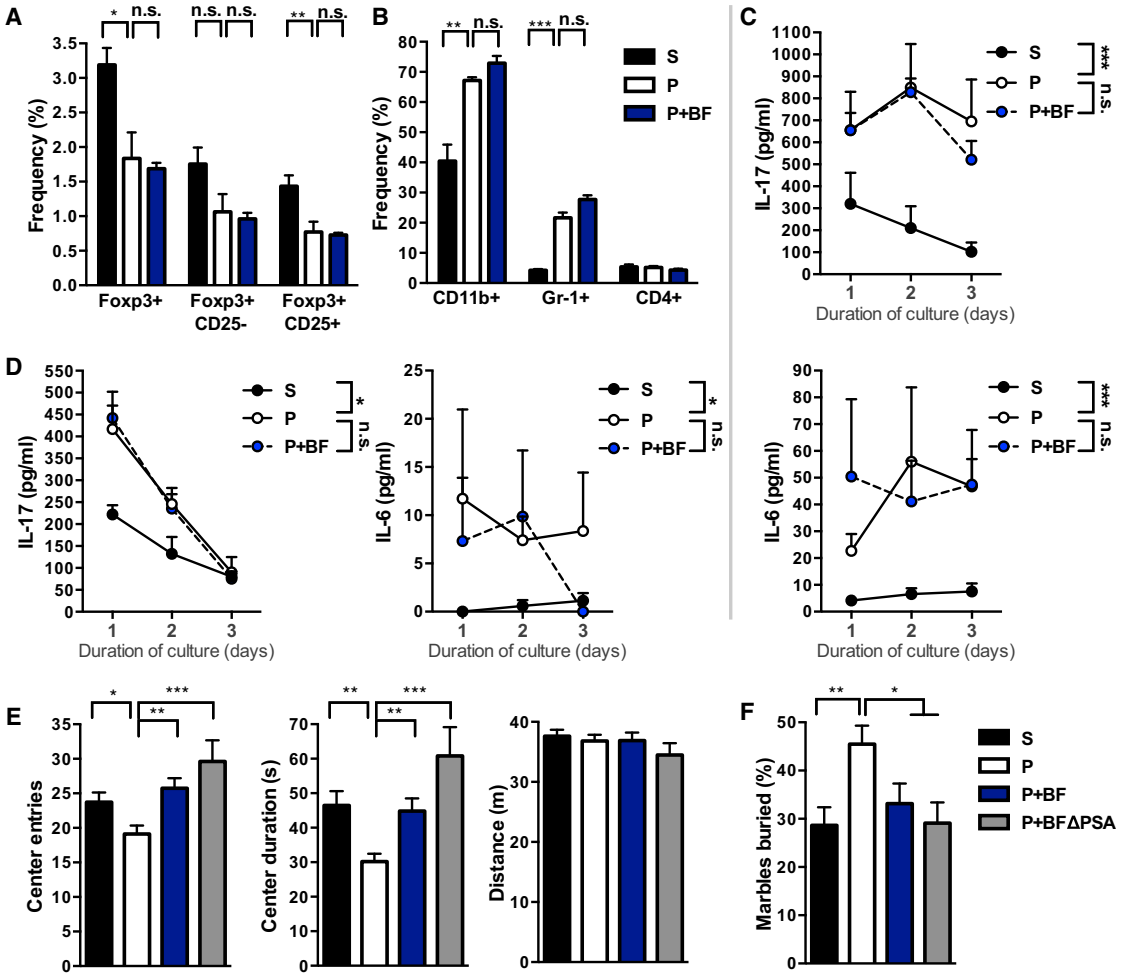

Figure S3. *B. fragilis* Treatment Has No Effect on Systemic Immune Dysfunction in MIA Offspring, Related to Figure 5

(A) Percent frequency of Foxp3+ CD25+ T regulatory cells from a parent population of CD4+ TCRb+ cells, measured by flow cytometry of splenocytes from adult saline, poly(I:C) and poly(I:C)+*B. fragilis* offspring. n = 5/group.

(B) Percent frequency of CD4+ T helper cells and CD11b+ and Gr-1+ neutrophilic and monocytic cells from a parent population of TER119- cells, measured by flow cytometry of splenocytes from adult saline, poly(I:C) and poly(I:C)+*B. fragilis* offspring. n = 5/group.

(C) Production of IL-17 and IL-6 by splenic CD4+ T cells isolated from adult saline and poly(I:C) offspring, after in vitro stimulation with PMA/ionomycin. Treatment effects were assessed by repeated-measures two-way ANOVA with Bonferroni post hoc test. n = 5/group.

(D) Production of IL-17 and IL-6 by CD4+ T cells isolated from mesenteric lymph nodes of adult saline and poly(I:C) offspring, after in vitro stimulation with PMA/ionomycin. Treatment effects were assessed by repeated-measures two-way ANOVA with Bonferroni post hoc test. n = 5/group.

(E) Anxiety-like and locomotor behavior in the open field exploration assay for adult MIA offspring treated with mutant *B. fragilis* lacking production of polysaccharide A (PSA). Data indicate total distance traveled in the 50 × 50 cm open field (right), duration spent in the 17 x17 cm center square (middle) and number of entries into the center square (left) over a 10 min trial. Data for saline, poly(I:C) and poly(I:C)+*B. fragilis* groups are as in Figure 5. poly(I:C)+*B. fragilis* with PSA deletion: n = 17.

(F) Repetitive burying of marbles in a 6 × 8 array in a 10 min trial. Data for saline, poly(I:C) and poly(I:C)+*B. fragilis* groups are as in Figure 5. poly(I:C)+*B. fragilis* with PSA deletion: n = 17.

Data are presented as mean ± SEM. *p < 0.05, **p < 0.01, ***p < 0.001. S = saline+vehicle, p = poly(I:C)+vehicle, P+BF = poly(I:C)+*B. fragilis*, P+BFΔPSA = poly(I:C)+*B. fragilis* with PSA deletion.

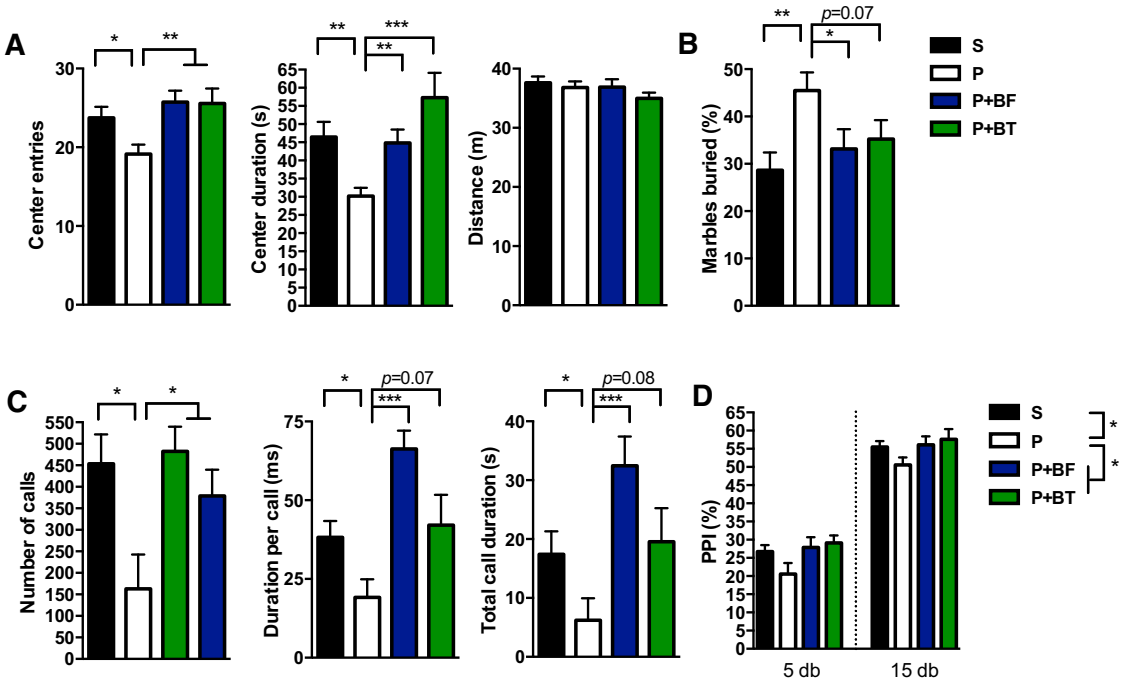

Figure S4. Amelioration of Autism-Related Behaviors in MIA Offspring Is Not Specific to *B. fragilis* Treatment, Related to Figure 5

(A) Anxiety-like and locomotor behavior in the open field exploration assay, as measured by total distance traveled in the 50 × 50 cm open field (right), duration spent in the 17 x17 cm center square (middle), and number of entries into the center of the field (left) over a 10 min trial. Poly(I:C)+*B. thetaiotaomicron*: n = 32.

(B) Repetitive burying of marbles in a 3 × 6 array during a 10 min trial. Poly(I:C)+*B. thetaiotaomicron*: n = 32.

(C) Communicative behavior, as measured by total number (left), average duration (middle) and total duration (right) of ultrasonic vocalizations produced by adult male mice during a 10 min social encounter. Poly(I:C)+*B. thetaiotaomicron*: n = 10.

(D) Sensorimotor gating in the PPI assay, as measured by percent difference between the startle response to pulse only and startle response to pulse preceded by a 5 db or 15 db prepulse. Treatment effects were assessed by repeated-measures two-way ANOVA with Bonferroni post hoc test. Poly(I:C)+*B. thetaiotaomicron*: n = 32.

For all panels, data for saline, poly(I:C) and poly(I:C)+*B. fragilis* are as in Figure 5. Graphs represent cumulative results obtained for 3-6 independent cohorts of mice. Data are presented as mean ± SEM. *p < 0.05, **p < 0.01, ***p < 0.001. S = saline+vehicle, p = poly(I:C)+vehicle, P+BF = poly(I:C)+*B. fragilis*, P+BT = Poly(I:C)+B. *thetaiotaomicron*.

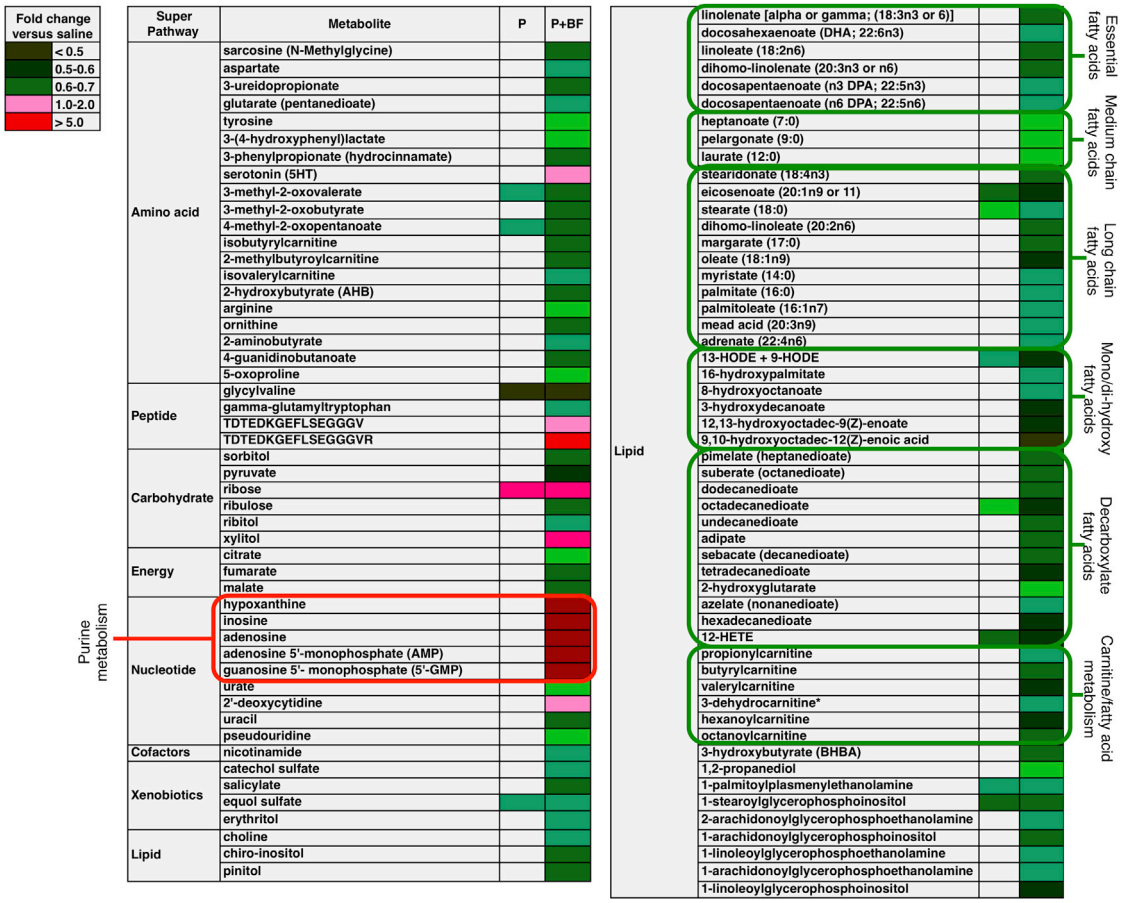

Figure S5. *B. Fragilis* Treatment Causes Statistically Significant Alterations in Serum Metabolites, with Widespread Changes in Biochemicals Relevant to Fatty Acid Metabolism and Purine Salvage Pathways, Related to Figure 6

Levels of 103 metabolites that are significantly altered in sera of *B. fragilis*-treated MIA offspring compared to saline controls, as measured by GC/LC-MS. Colors indicate fold change relative to metabolite concentrations detected in saline offspring, where red hues represent increased levels compared to controls and green hues represent decreased levels compared to controls (see legend on top left). All changes indicated are $p < 0.05$ by two-way ANOVA with contrasts. p = poly(I:C), P+BF = poly(I:C)+*B. fragilis*. n = 8/group.

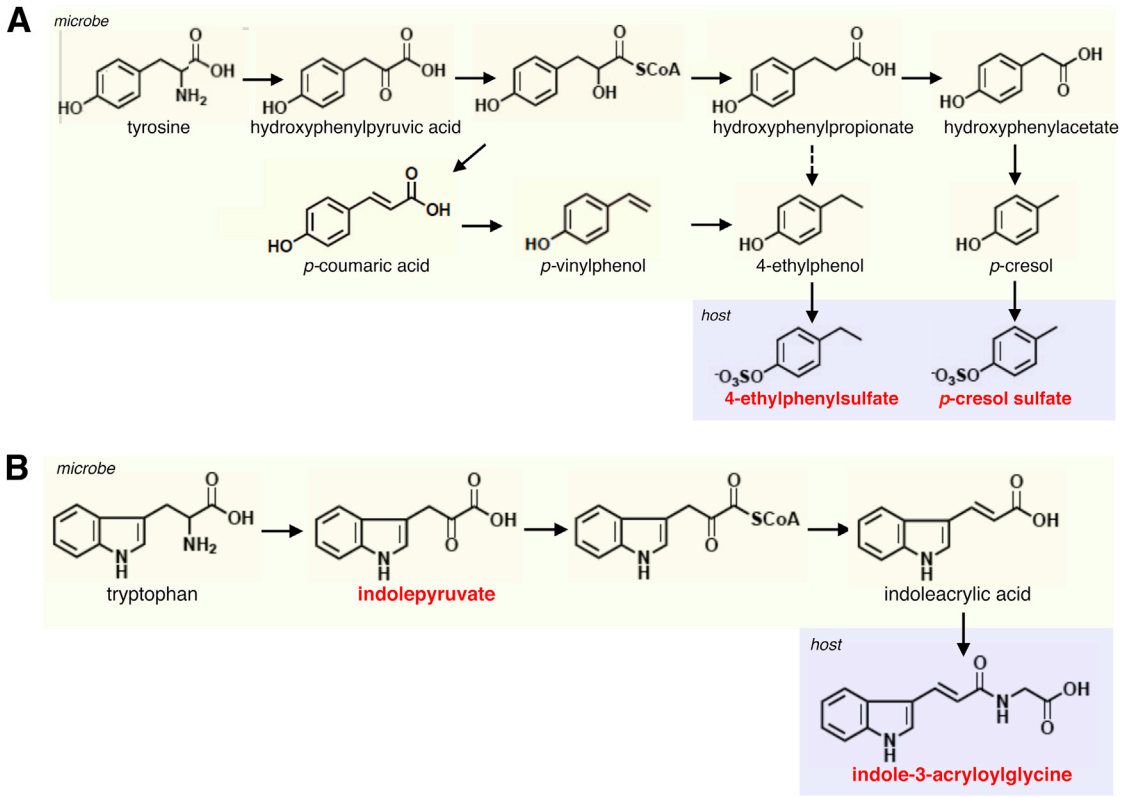

Figure S6. Synthesis of Autism-Associated Metabolites by Host-Microbe Interactions, Related to Figure 6

(A) Diagram illustrating the synthesis of 4EPS (found elevated in MIA serum and restored by *B. fragilis* treatment) and *p*-cresol (reported to be elevated in urine of individuals with ASD) by microbial tyrosine metabolism and host sulfation.

(B) Diagram illustrating the synthesis of indolepyruvate (found elevated in MIA serum and restored by *B. fragilis* treatment) and indole-3-acryloylglycine (reported to be elevated in urine of individuals with ASD) from microbial tryptophan metabolism and host glycine conjugation.

Solid arrows represent known biological conversions. Dotted arrow represents predicted biological conversions.

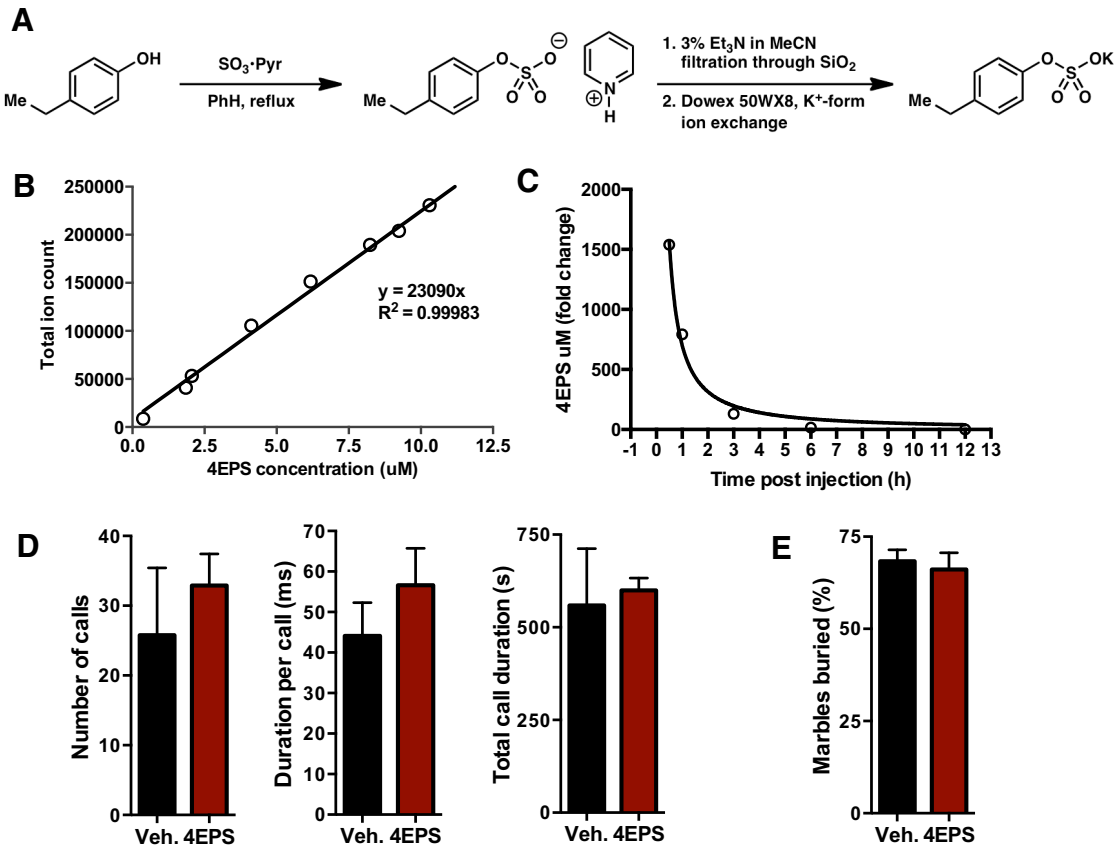

Figure S7. 4-ethylphenylsulfate Synthesis, Detection and In Vivo Experiments, Related to Figure 6

(A) Diagram of 4EPS synthesis by treating 4-ethylphenol with sulfur trioxide-pyridine in refluxing benzene to generate the pyridinium salt followed by ion exchange over K+ resin to generate the potassium salt.

(B) Dose-response curve and linear regression analysis for known concentrations of potassium 4EPS analyzed by LC/MS.

(C) Time-dependent increases in serum 4EPS after a single i.p. injection of 30 mg/kg potassium 4EPS into adult wild-type mice.

(D) Communicative behavior, as measured by total number (left), average duration (middle) and total duration (right) of ultrasonic vocalizations produced by adult male mice during a 10 min social encounter. n = 5/group.

(E) Repetitive burying of marbles in a 3 × 6 array during a 10 min trial. n = 10/group.

Data are presented as mean ± SEM. Veh. = vehicle (saline), 4EPS = 4-ethylphenylsulfate.